AIP | Applied Physics Letters

Resistance switching in epitaxial SrCoO x thin films

Octolia T. Tambunan, Kadek J. Parwanta, Susant K. Acharya, Bo Wha Lee, Chang Uk Jung, Yeon Soo Kim, Bae Ho Park, Huiseong Jeong, Ji-Yong Park, Myung Rae Cho, Yun Daniel Park, Woo Seok Choi, Dong-Wook Kim, Hyunwoo Jin, Suyoun Lee, Seul Ji Song, Sung-Jin Kang, Miyoung Kim, and Cheol Seong Hwang

Citation: Applied Physics Letters **105**, 063507 (2014); doi: 10.1063/1.4893323
View online: http://dx.doi.org/10.1063/1.4893323
View Table of Contents: http://scitation.aip.org/content/aip/journal/apl/105/6?ver=pdfcov
Published by the AIP Publishing

Resistance switching in epitaxial $SrCoO_x$ thin films

Octolia T. Tambunan,[1] Kadek J. Parwanta,[1] Susant K. Acharya,[1] Bo Wha Lee,[1] Chang Uk Jung,[1,a)] Yeon Soo Kim,[2] Bae Ho Park,[2] Huiseong Jeong,[3] Ji-Yong Park,[3] Myung Rae Cho,[4] Yun Daniel Park,[4] Woo Seok Choi,[5] Dong-Wook Kim,[6] Hyunwoo Jin,[7] Suyoun Lee,[7] Seul Ji Song,[8] Sung-Jin Kang,[8] Miyoung Kim,[8] and Cheol Seong Hwang[8]
[1]*Department of Physics, Hankuk University of Foreign Studies, Yongin 449-791, South Korea*
[2]*Division of Quantum Phases and Devices, Department of Physics, Konkuk University, Seoul 143-791, South Korea*
[3]*Department of Physics and Division of Energy System Research, Ajou University, Suwon 443-749, South Korea*
[4]*Department of Physics and Astronomy and Center for Subwavelength Optics, Seoul National University, Seoul 151-747, South Korea*
[5]*Department of Physics, Sungkyunkwan University, Suwon 440-746, South Korea*
[6]*Department of Physics, Ewha Womans University, Seoul 120-750, South Korea*
[7]*Electronic Materials Research Center, Korea Institute of Science and Technology, Seoul 136-791, South Korea*
[8]*Department of Material Science and Engineering, Seoul National University, Seoul 151-747, South Korea*

(Received 7 May 2014; accepted 4 August 2014; published online 14 August 2014)

We observed bipolar switching behavior from an epitaxial strontium cobaltite film grown on a $SrTiO_3$ (001) substrate. The crystal structure of strontium cobaltite has been known to undergo topotactic phase transformation between two distinct phases: insulating brownmillerite ($SrCoO_{2.5}$) and conducting perovskite ($SrCoO_{3-\delta}$) depending on the oxygen content. The current–voltage characteristics of the strontium cobaltite film showed that it could have a reversible insulator-to-metal transition triggered by electrical bias voltage. We propose that the resistance switching in the $SrCoO_x$ thin film could be related to the topotactic phase transformation and the peculiar structure of $SrCoO_{2.5}$. © *2014 AIP Publishing LLC*. [http://dx.doi.org/10.1063/1.4893323]

Recently, strontium cobaltite ($SrCoO_x$; SCO) has attracted much attention for its rich phase diagram and high oxygen mobility, even at room temperature,[1–4] as well as its catalytic activity.[5] Depending on its oxygen stoichiometry, the crystal structure of SCO exhibits a topotactic phase transformation between two distinct phases: brownmillerite $SrCoO_{2.5}$ (BM-SCO) and perovskite $SrCoO_{3-\delta}$ (P-SCO). BM-SCO has an orthorhombic unit cell ($a_o = 5.574$ Å; $b_o = 5.470$ Å; $c_o = 15.745$ Å),[4] which can be represented by a pseudo-tetragonal structure ($a_t = 3.905$ Å; $c_t/4 = 3.936$ Å), while P-SCO has a cubic perovskite configuration ($a_c = 3.829$ Å).[6] BM-SCO is an antiferromagnetic insulator, whereas P-SCO is a ferromagnetic metal. Reversible topotactic phase changes between BM-SCO and P-SCO have been reported in bulk samples using a liquid-electrolyte-based electrochemical cell,[2,3] as well as in thin-film samples via *ex-situ* chemical oxidation,[7,8] *in-situ* high-oxygen-pressure annealing,[9] and *ex-situ* low-temperature annealing under suitable gas conditions.[10,11]

Reversible changes between a high resistance state (HRS) and a low resistance state (LRS) in many transition metal-oxide materials have been understood in terms of resistance-switching phenomena.[12] By applying appropriate writing voltage pulses, a cell in its HRS can be "SET" to a LRS, then again "RESET" back to a HRS. Most accept that ionic transport and electrochemical redox reactions provide the essential mechanism for resistive switching in oxide materials containing transition-metal ions that display bipolar resistance switching (BRS) behaviors.[13–15] The possible driving mechanisms for resistance switching can be classified as filamentary type or interface type,[16] although the clear distinction becomes blurred as the size of the memory cell approaches the filament diameter ($<10 \times 10\,nm^2$). A variety of transition-metal oxides have shown resistance-switching behavior, including $SrTiO_3$,[17] TiO_2,[18] NiO,[19] and $Pr_{0.7}Ca_{0.3}MnO_3$.[20] Co-based materials, such as CoO,[21] Co_3O_4,[22–24] Co-doped ZnO, and Co-doped $BaTiO_3$,[25,26] have also shown this behavior. The resistance-switching mechanism in Co-based oxide materials is based mostly on the filamentary conducting-path model, caused by some combination of varied valencies of Co, oxygen migration, and local reduction–oxidation of cobalt oxide.

In this paper, we report the reversible transition of the resistance in a SCO film, grown on a $SrTiO_3$ (STO) (001) substrate, from an insulating state to a conducting state, triggered by an external electrical bias voltage. Among Co-based oxide materials, SCO has high oxygen mobility even at room temperature. It also demonstrates rapid reversible redox activity that may result in an unusual resistance-switching mechanism that has not yet been observed in other materials. Resistance switching under an applied voltage has yet to be reported for SCO materials.

Figure 1(a) shows a schematic of our device structure. First, we deposited an epitaxial $SrRuO_3$ (SRO) bottom electrode (BE) layer (thickness: 60 nm) on a STO (001) substrate, using pulsed laser deposition (PLD) at a substrate temperature of 750 °C. A KrF excimer laser (repetition rate: 4 Hz; fluence: ~2.5 J cm^{-2}) was used for PLD. The resulting SRO layer exhibited coherent growth, with an out-of-plane lattice constant of 3.955 Å.[27–29] Photolithography and etching were used to fabricate patterned SRO as a BE.

a)Email: cu-jung@hufs.ac.kr

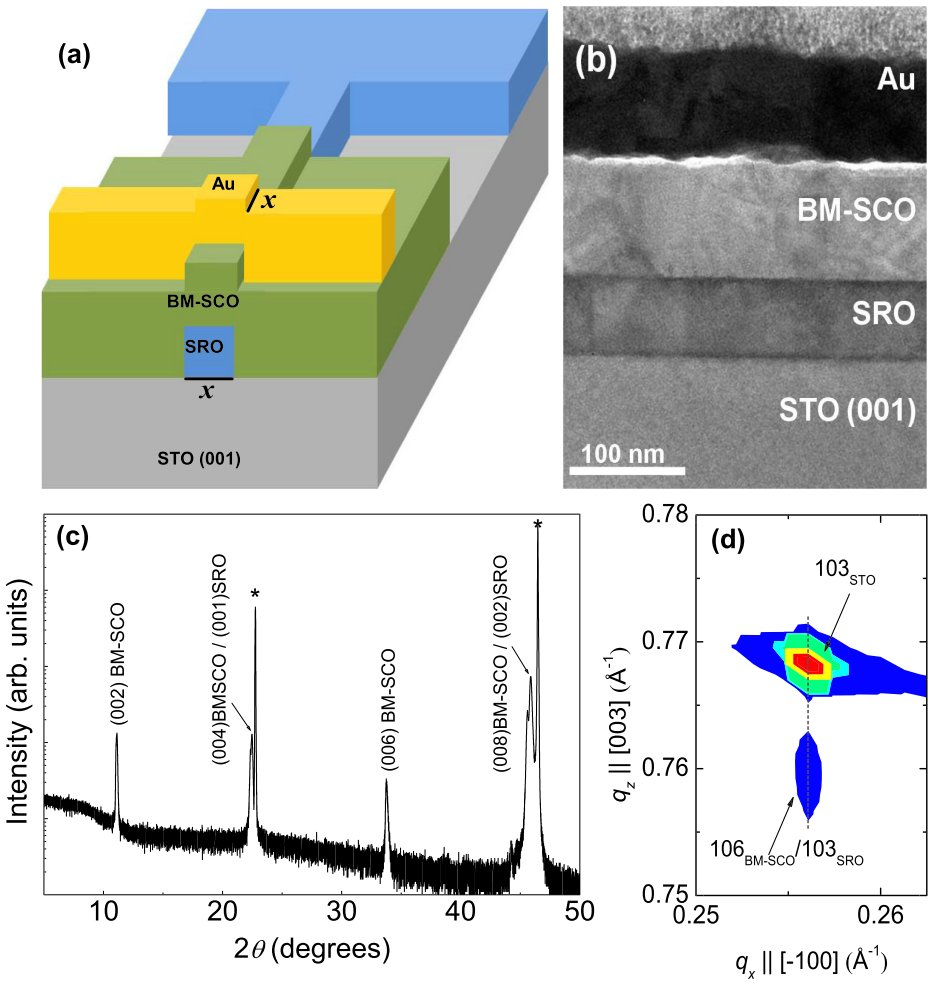

FIG. 1. (a) Schematic of the Au/BM-SCO/SRO/STO (001) cross-point device structure (BM-SCO: $SrCoO_{2.5}$; SRO: $SrRuO_3$; STO: $SrTiO_3$). The line width (x) was 10, 20, 40, or 80 μm. (b) Cross-sectional TEM images of the Au/BM-SCO/SRO/STO (001) cross-point cell. (c) X-ray diffraction $\theta-2\theta$ patterns of BM-SCO/SRO/STO (001) thin films. The STO substrate peaks are indicated with asterisks. (d) Reciprocal space maps near the (103) STO Bragg reflection.

A BM-SCO film (thickness: 100 nm) was deposited on the patterned SRO layer by PLD at a substrate temperature of 600 °C, using a ceramic BM-SCO target. Photolithography was performed again to pattern the top electrode (TE). Finally, an Au-patterned layer (thickness: 80 nm) was deposited using electron-beam evaporation. The patterned SRO and Au TE had varied line widths of 10, 20, 40, and 80 μm, resulting in a cell area of 100–6400 μm^2. Such a simple cross-point device can effectively reduce the active area, because switching only takes places within the current path defined by the line width of Au and SRO.[30] We investigated the structure of the fabricated Au/BM-SCO/SRO/STO (001) device by using transmission electron microscopy (TEM, JEOL 2100FS). The cross-sectional TEM images of the cell in Fig. 1(b) show smooth sharp boundaries between layers.

High-resolution X-ray diffraction (Bruker D8 Discover) was performed to investigate the epitaxial structure of the BM-SCO/SRO/STO (001) film. Figure 1(c) shows the $\theta-2\theta$ patterns of the unpatterned BM-SCO/SRO/STO (001) thin film. The diffraction peak of the (008) planes of BM-SCO overlapped with the peak corresponding to the (002) planes of SRO. The average lattice constant of the BM-SCO film, calculated from the (002), (004), (006), and (008)-BM-SCO peaks, was 3.951 Å. No other Bragg diffraction peaks besides those associated with the film appeared, suggesting the oxide structure was phase-pure and hetero-epitaxial. X-ray rocking-curve analysis of the peaks revealed a full-width at half-maximum (FWHM) $< 0.07°$, indicating the films were highly crystalline (in comparison, the FWHM of the STO peaks was $\sim 0.02°$) (data not shown). The reciprocal space maps shown in Fig. 1(d) confirm the fully strained growth of the BM-SCO/SRO film on the STO (001) substrate, with the same in-plane lattice constant to STO (100) substrate.

Electrical testing was performed using an Agilent B1540 semiconductor-device analyzer at room temperature. Temperature-dependent resistivity was measured over 10–300 K by using a Keithley 2636 source-measure unit and a CS202*I-DMX-1SS cryogenic system. During these measurements, a bias voltage was applied to the TE, while the BE remained grounded.

Figure 2(a) shows typical current–voltage (I–V) curves obtained during resistance switching of Au/BM-SCO/SRO cross-point cells, each with a cell area of 100 μm^2. Initially, their resistance was high, suggesting that the BM-SCO film was insulating. As the voltage swept to a positive bias, at 1 V the current suddenly increased, switching the device to the LRS; this is referred to as the forming process. As the voltage then swept to a negative bias to about −2.1 V, the current decreased, resetting the device to the HRS. The LRS could be obtained again, but at a higher voltage ($\sim$2 V). Hereafter, we observed stable bipolar resistance switching, at least up to 30 switching cycles. In general, the forming step created a filamentary conducting path via soft breakdown of the insulating pristine film.[15,16]

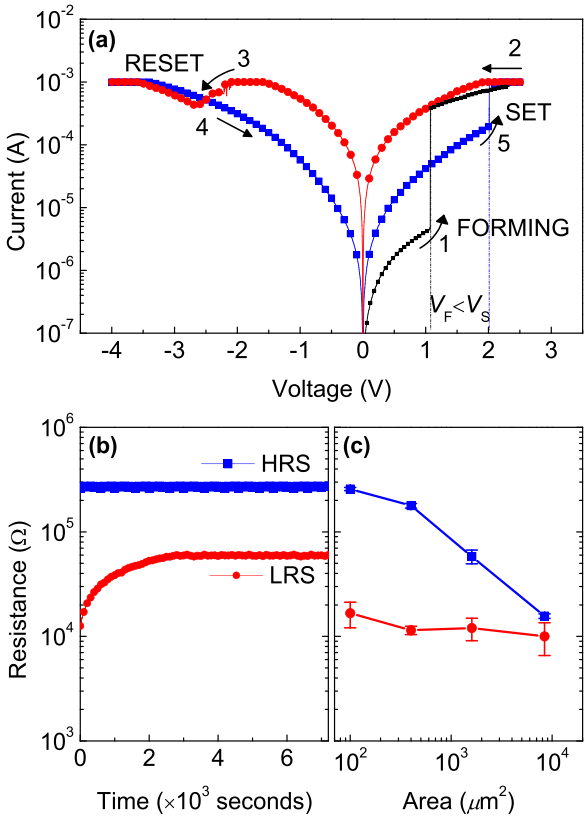

FIG. 2. (a) Current–voltage (*I*–*V*) curves of the Au/BM-SCO/SRO cross-point cell. The arrows indicate the direction of the voltage sweep. (b) Retention data and (c) cell-area dependence of the low-resistance state (LRS) and high-resistance state (HRS) after the SET and RESET steps.

The forming voltage (V_F) being higher than the set voltage (V_S) can be problematic for operating integrated devices; however, $V_F \sim V_S$ is possible in several cases.[15] The observation of $V_F < V_S$ in our device indicates that SCO may have an unusual resistance-switching mechanism that could be favorable for device operation. We will discuss possible reasons for this unusual switching later.

The retention time of the device was measured with a bias voltage of 0.2 V, as shown in Fig. 2(b). The resistance of the LRS initially decayed over the first 2×10^3 s, but maintained its resistance thereafter for $>7 \times 10^3$ s without further significant decay. Figure 2(c) shows the resistances of the LRS and the HRS for cells with different cell areas. As the cell area increased, the LRS resistance remained about constant, while the HRS resistance depended much on area. For cells with areas $>80 \times 80\,\mu m^2$, the switching behavior practically disappeared, possibly because of high leakage current. The resistance cell–area relationship is an indirect approach used to demonstrate the switching mechanism.[31] The weak dependence of the LRS resistance on cell area suggests that the Au/BM-SCO/SRO switching mechanism was the filamentary conducting path model.[31] The area-dependent current of the HRS implies that the leakage current flowed uniformly across the entire area of the memory cell.

The relationship between the different resistance states and the local crystal structure can best be revealed by microscopic examination of the LRS/HRS crystal structure using *ex-situ* TEM, or *in-situ* TEM for some oxides.[32] However, TEM of the P-SCO phase was not plausible in the present work because the electron-beam shower under high-vacuum conditions for TEM imaging disturbs SCO and changes P-SCO into BM-SCO. In place of TEM, we used an indirect method: measuring the temperature-dependent transport properties of BM-SCO, Mix-SCO (a mixture of BM-SCO and P-SCO), and P-SCO; this method is described in a previous study for homogenous thin films (size: 5×5 mm).[9]

Figure 3 shows resistivity–temperature curves ($\rho(T)$) for the LRS and HRS of our device; $\rho(T)$ for BM-, Mix-, and P-SCO thin-films, as reported by Jeen *et al.*, are also shown for comparison.[9] The measured $\rho(T)$ in the LRS of our device was comparable both in temperature behavior and resistivity with the reported Mix-SCO. The calculated thermal activation energy of the LRS was 7 meV. The $\rho(T)$ in the HRS shows highly insulating behavior, with a slightly lower resistivity than that of BM-SCO. The calculated thermal activation energy of the HRS of our device was 0.17 eV, comparable to the activation energy of the BM-SCO thin film (0.19 eV).[9] This similarity indicates that the HRS cell had electrical properties similar to the BM-SCO film. Our pristine-state device exhibited similar $\rho(T)$ behavior with larger magnitude, revealing that it has identical physical properties to those reported for BM-SCO.

It was reported that the $\rho(T)$ of the BM-SCO showed highly insulating behavior, but that Mix-SCO and P-SCO showed semiconductor-like behavior rather than metal-like behavior. The semiconductor-like behavior originates from the lack of long-range order caused by incomplete oxidation. Similar $\rho(T)$ characteristics have also been observed in $SrFeO_x$ thin films having the same topotactic structure transition as SCO.[33] A very slight decrease in the oxygen stoichiometry in $SrCoO_3$ and $SrFeO_3$ maintains the perovskite phase but produces semiconductor-like behavior, although the absolute resistivity is much smaller than that in purely insulating brownmillerite $SrCoO_{2.5}$ and $SrFeO_{2.5}$. Moreover, Jeen *et al.* measured the $\rho(T)$ of "microscale" homogenous, planar SCO thin films,[9] while our devices consist of filaments, contained in a matrix phase, that have vertical geometry for current flow. The differences between these two measurements in the current path and microscale homogeneity may

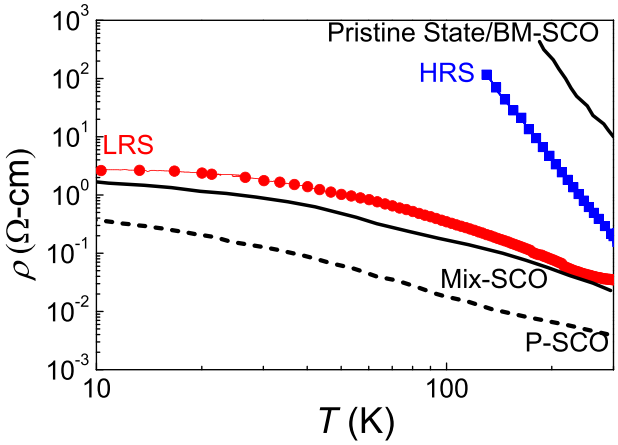

FIG. 3. Temperature-dependent resistivity for the LRS and HRS. Data from the current study (shown by the line with symbols) are compared with previously reported data for BM-SCO, Mix-SCO, and P-SCO.[9]

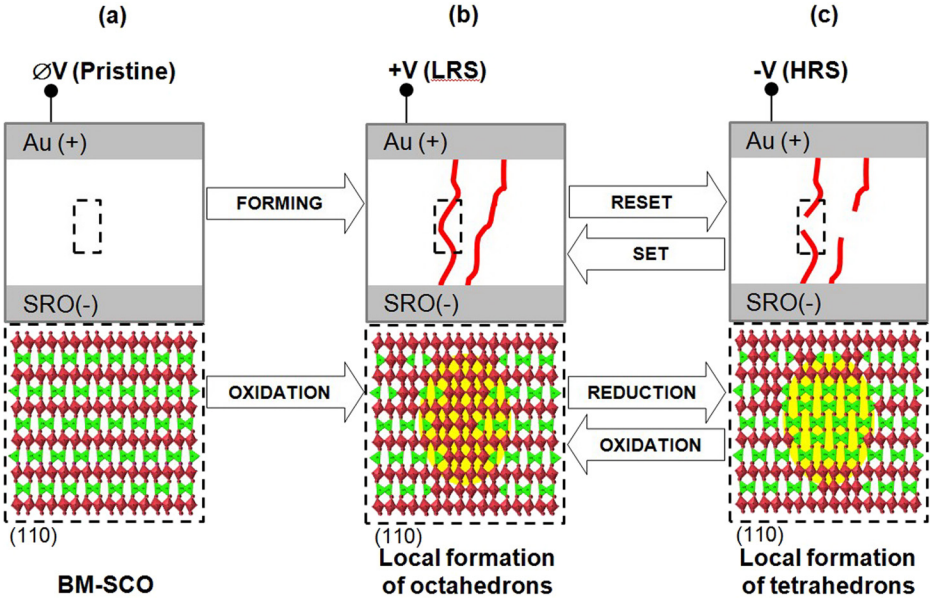

FIG. 4. Schematic view of the filament model as a resistance-switching mechanism (upper panel) and the topotactic phase transformation of SCO caused by external bias-voltage-induced, reversible redox activity (lower panel). (a) Pristine state showing the peculiar structure, consisting of two sub-layers: an octahedral layer (shown in red) and a tetrahedral layer (shown in green). (b) LRS made by oxygenating a few tetrahedrons between two adjacent octahedral layers. (c) HRS made by deoxygenating octahedrons over a wider area from the sudden HRS switching.

have led to somewhat different absolute resistances. Although we did not observe clear metallic behavior from the perovskite phase, and though the measurement geometry differed, the different $\rho(T)$ characteristics of the BM- and P-SCO phases are still useful for estimating the local crystal structure in the different resistance states.

In the conventional filamentary mechanism, filament formation (electroforming) is essentially a soft dielectric breakdown that occurs all the way from the BE to TE; electroforming essentially builds a long conducting bridge between the BE and TE. This differs from the set and reset processes that occur after electroforming, because only a short segment of the filamentary path disconnects and reconnects repeatedly.[13,15] Thus, electroforming generally requires a voltage higher than the set voltage ($V_S < V_F$). For SCO, the forming voltage required to change from the pristine state to the LRS was significantly lower than the set voltage ($V_F < V_S$), and the pristine state was more insulating than the HRS. To understand the resistance switching in this material system, the crystal structure of BM-SCO must be understood in detail.

Figure 4 shows a schematic explanation of a viable filament model for the resistance-switching mechanism (upper panel) and the topotactic phase transformation of the SCO film (lower panel) in this study. The BM-SCO is a structurally ordered insulator that has its out-of-plane carrier transportation interrupted by the layered crystal structure. Insulating BM-SCO consists of alternately stacked, fully oxygenated octahedral sub-layers and oxygen-deficient tetrahedral sub-layers, with Co^{4+} and Co^{2+}, respectively,[5,9,10] as shown in Fig. 4(a). Thus, changing the pristine state to the LRS would only require placing "conducting stepping stones" (oxygen ions) between the closely spaced, fully oxygenated octahedral sub-layers, rather than creating the long conducting bridge.

Initially, when a positive electric bias voltage is applied to pristine BM-SCO, the oxygen ions drift from the SRO-BE into the BM-SCO. Because the CoO_6 octahedrons are already fully oxygen coordinated, the injected oxygen ions must be incorporated into the layers with CoO_4 tetrahedrons. As a consequence, some of the tetrahedral sites must change to octahedral sites. Ion drift in resistance switching is generally assisted by Joule heating, which must occur at local sites where electronic carrier injection is high, causing oxygen "stuffing." This process eventually forms localized conducting filaments in BM-SCO, wherein the structure is mostly P-SCO. The filaments increase the electrical conductivity of the sample, electroforming the sample. When a negative bias is applied, many of these stuffed oxygen ions drift back to the SRO electrode, which allows the samples to RESET. However, we can reasonably assume the drifting back of oxygen ions does not guarantee that the BM-SCO structure recovers, but instead creates clustered tetrahedrons (Fig. 4(c)). When the positive bias is then applied to SET the sample again, the increased tetrahedron density may require even greater migration of oxygen ions to convert the tetrahedrons to octahedrons (Fig. 4(b)) and to build a vertically connected octahedron chain; this requires a higher voltage than before, making $V_F < V_S$. The peculiar structure of BM-SCO and the suddenness of the RESET process can explain our observation that $V_F < V_S$ and that our SCO device's pristine state was more insulating than its HRS.

In summary, we found and evaluated bipolar resistive switching in Au/BM-SCO/SRO/STO (001) devices. The different temperature dependent resistivity behaviors between the LRS and HRS suggest that the bipolar resistive switching of the memory cell might originate from a local reversible-phase transformation from BM-SCO to Mix-SCO. Unlike in most switching devices, the electroforming voltage required to change from the pristine state to the LRS was significantly lower than the SET voltage in our device. To explain these behaviors, we proposed a viable switching mechanism based on the topotactic phase transformation of SCO. The unique structure of BM-SCO and the unexpected behavior of the RESET process support this hypothesis. This reversible-phase transformation in SCO triggered by a bias voltage could make it useful as resistive random-access memory.

We thank C. Liu for helpful discussion. This work was supported by Basic Science Research Program through

the National Research Foundation of Korea (NRF) funded by the Ministry of Education, Science and Technology (2012R1A1A2008595, 2012R1A1A2008845, and 2013R1 A2A2A01067415). B.H.P. was supported by the NRF (2013R1A3A2042120), Y.D.P. and M.R.C. were supported by the NRF (2014-023563 and 2008-0061906), W.S.C. was supported by Samsung Research Fund, Sungkyunkwan University, 2013, and C.S.H. was supported by the Global Research Laboratory Program (2012040157) of NRF. H.J. and S.L. gratefully acknowledged the financial support of the Korea Institute of Science and Technology (KIST) through 2E24881 and 2V03330.

[1]T. Takeda, Y. Yamaguchi, and H. Watanabe, J. Phys. Soc. Jpn. **33**, 970 (1972).
[2]A. Nemudry, P. Rudolf, and R. Schöllhorn, Chem. Mater. **8**, 2232 (1996).
[3]R. Le Toquin, W. Paulus, A. Cousson, C. Prestipino, and C. Lamberti, J. Am. Chem. Soc. **128**, 13161 (2006).
[4]A. Muñoz, C. de la Calle, J. A. Alonso, P. M. Botta, V. Pardo, D. Baldomir, and J. Rivas, Phys. Rev. B **78**, 054404 (2008).
[5]H. Jeen, Z. Bi, W. S. Choi, M. F. Chisholm, C. A. Bridges, M. P. Paranthaman, and H. N. Lee, Adv. Mater. **25**, 6459 (2013).
[6]Y. Long, Y. Kaneko, S. Ishiwata, Y. Taguchi, and Y. Tokura, J. Phys.: Condens. Matter **23**, 245601 (2011).
[7]N. Ichikawa, M. Iwanowska, M. Kawai, C. Calers, W. Paulus, and Y. Shimakawa, Dalton Trans. **41**, 10507 (2012).
[8]O. T. Tambunan, M. Y. Lee, D. H. Kim, K. J. Parwanta, and C. U. Jung, J. Korean Phys. Soc. **64**, 1845 (2014).
[9]H. Jeen, W. S. Choi, J. W. Freeland, H. Ohta, C. U. Jung, and H. N. Lee, Adv. Mater. **25**, 3651 (2013).
[10]H. Jeen, W. S. Choi, M. D. Biegalski, C. M. Folkman, I.-C. Tung, D. D. Fong, J. W. Freeland, D. Shin, H. Ohta, M. F. Chisholm, and H. N. Lee, Nat. Mater. **12**, 1057 (2013).
[11]W. S. Choi, H. Jeen, J. H. Lee, S. S. A. Seo, V. R. Cooper, K. M. Rabe, and H. N. Lee, Phys. Rev. Lett. **111**, 097401 (2013).
[12]R. Waser, *Nanoelectronics and Information Technology* (Wiley-VCH, Weinheim, 2003), p. 257.
[13]R. Waser and M. Aono, Nat. Mater. **6**, 833 (2007).
[14]R. Waser, R. Dittmann, G. Staikov, and K. Szot, Adv. Mater. **21**, 2632 (2009).
[15]K. M. Kim, D. S. Jeong, and C. S. Hwang, Nanotechnology **22**, 254002 (2011).
[16]A. Sawa, Mater. Today **11**, 28 (2008).
[17]K. Szot, W. Speier, G. Bihlmayer, and R. Waser, Nat. Mater. **5**, 312 (2006).
[18]B. J. Choi, D. S. Jeong, S. K. Kim, C. Rohde, S. Choi, J. H. Oh, H. J. Kim, C. S. Hwang, K. Szot, R. Waser, B. Reichenberg, and S. Tiedke, J. Appl. Phys. **98**, 033715 (2005).
[19]K. M. Kim, B. J. Choi, S. J. Song, G. H. Kim, and C. S. Hwang, J. Electrochem. Soc. **156**, G213 (2009).
[20]A. Sawa, T. Fujii, M. Kawasaki, and Y. Tokura, Appl. Phys. Lett. **85**, 4073 (2004).
[21]H. Shima, F. Takano, H. Muramatsu, H. Akinaga, Y. Tamai, I. H. Inque, and H. Takagi, Appl. Phys. Lett. **93**, 113504 (2008).
[22]K. Nagashima, T. Yanagida, K. Oka, M. Taniguchi, T. Kawai, J.-S. Kim, and B. H. Park, Nano Lett. **10**, 1359 (2010).
[23]X. Gao, H. Guo, Y. Xia, J. Yin, and Z. Liu, Thin Solid Films **519**, 450 (2010).
[24]A. Younis, D. Chu, X. Lin, J. Lee, and S. Li, Nanoscale Res. Lett. **8**, 36 (2013).
[25]Z. Yan, Y. Guo, G. Zhang, and J.-M. Liu, Adv. Mater. **23**, 1351 (2011).
[26]G. Chen, C. Song, C. Chen, S. Gao, F. Zeng, and F. Pan, Adv. Mater. **24**, 3515 (2012).
[27]C. U. Jung, H. Yamada, M. Kawasaki, and Y. Tokura, Appl. Phys. Lett. **84**, 2590 (2004).
[28]B. W. Lee, C. U. Jung, M. Kawasaki, and Y. Tokura, J. Appl. Phys. **104**, 103909 (2008).
[29]B. Lee, O.-U. Kwon, R. H. Shin, W. Jo, and C. U. Jung, Nanoscale Res. Lett. **9**, 8 (2014).
[30]I. G. Baek, D. C. Kim, M. J. Lee, H.-J. Kim, E. K. Yim, M. S. Lee, J. E. Lee, S. E. Ahn, S. Seo, J. H. Lee, J. C. Park, Y. K. Cha, S. O. Park, H. S. Kim, I. K. Yoo, U.-I. Chung, J. T. Moon, and B. I. Ryu, Tech. Dig. - Int. Electron. Devices Meet. **2005**, 750.
[31]X.-J. Zhu, J. Shang, and R.-W. Li, Front. Mater. Sci. **6**, 183 (2012).
[32]D.-H. Kwon, K. M. Kim, J. H. Jang, J. M. Jeon, M. H. Lee, G. H. Kim, X.-S. Li, G.-S. Park, B. Lee, S. Han, M. Kim, and C. S. Hwang, Nat. Nanotechnol. **5**, 148 (2010).
[33]H. Yamada, M. Kawasaki, and Y. Tokura, Appl. Phys. Lett. **80**, 622 (2002).